JB Journals.ASM.org

Bordetella parapertussis PagP Mediates the Addition of Two Palmitates to the Lipopolysaccharide Lipid A

L. E. Hittle,[a] J. W. Jones,[b] A. M. Hajjar,[c] R. K. Ernst,[a] A. Preston[d]

Department of Microbial Pathogenesis, University of Maryland School of Dentistry, Baltimore, Maryland, USA[a]; Department of Pharmaceutical Sciences, University of Maryland School of Pharmacy, Baltimore, Maryland, USA[b]; Department of Comparative Medicine, School of Medicine, University of Washington, Seattle, Washington, USA[c]; Department of Biology and Biochemistry, University of Bath, Bath, United Kingdom[d]

***Bordetella bronchiseptica* PagP ($PagP_{BB}$) is a lipid A palmitoyl transferase that is required for resistance to antibody-dependent complement-mediated killing in a murine model of infection. *B. parapertussis* contains a putative *pagP* homolog (encoding *B. parapertussis* PagP [$PagP_{BPa}$]), but its role in the biosynthesis of lipid A, the membrane anchor of lipopolysaccharide (LPS), has not been investigated. Mass spectrometry analysis revealed that wild-type *B. parapertussis* lipid A consists of a heterogeneous mixture of lipid A structures, with penta- and hexa-acylated structures containing one and two palmitates, respectively. Through mutational analysis, we demonstrate that $PagP_{BPa}$ is required for the modification of lipid A with palmitate. While $PagP_{BB}$ transfers a single palmitate to the lipid A C-3′ position, $PagP_{BPa}$ transfers palmitates to the lipid A C-2 and C-3′ positions. The addition of two palmitate acyl chains is unique to *B. parapertussis*. Mutation of $pagP_{BPa}$ resulted in a mutant strain with increased sensitivity to antimicrobial peptide killing and decreased endotoxicity, as evidenced by reduced proinflammatory responses via Toll-like receptor 4 (TLR4) to the hypoacylated LPS. Therefore, PagP-mediated modification of lipid A regulates outer membrane function and may be a means to modify interactions between the bacterium and its human host during infection.**

The genus *Bordetella* contains nine species, three of which have been studied in detail: *B. pertussis*, *B. parapertussis*, and *B. bronchiseptica*. *B. pertussis* and *B. parapertussis* are the causative agents of whooping cough. While long considered a disease of infants and children, it is now recognized that infections occur in adults, although they are milder than the classic whooping cough described in children (1–5). *B. pertussis* is considered the major pathogen of whooping cough; however, the prevalence of *B. parapertussis* in disease is not well understood but may be a significant contributor to the overall burden (6). Symptoms of *B. parapertussis* and *B. pertussis* disease are clinically indistinguishable and include a prolonged cough, whooping, paroxysms, vomiting, and cyanosis (7), leading to increased mortality in infected children; however, *B. parapertussis* is often considered to cause milder disease than *B. pertussis* (7). In many countries, whooping cough is controlled by vaccination against *B. pertussis*. However, many countries have recently suffered major outbreaks despite continuous high levels of vaccine coverage, initiating renewed interest in whooping cough vaccinology. The acellular pertussis vaccines (DTaP and Tdap) used in most developed countries do not result in protection against *B. parapertussis*, likely due to the *B. parapertussis* lipopolysaccharide (LPS) O antigen inhibiting the binding of antibodies to the bacterium (8).

LPS is the major component of the outer leaflet of the outer membrane of Gram-negative bacteria. The lipid A region imparts the endotoxin activity of LPS (9) that arises when lipid A binds to a host membrane complex that includes and activates signaling by Toll-like receptor 4 (TLR4) (10), resulting in the expression of many proinflammatory cytokines and chemokines in cells of the innate immune system. TLR4 signaling is also important for the activation of adaptive immunity, particularly through the activation of dendritic cells (DCs), which act as antigen-presenting cells (APCs) for T cells. Thus, lipid A-TLR4 interactions are central to the host immune response to Gram-negative bacteria, including *Bordetella* species.

Bordetella subspecies exhibit extensive heterogeneity in their lipid A structure, arising from both species-specific differences in and species-variable expression of specific lipid A-modifying enzymes (11, 12). Previously, we demonstrated that *B. bronchiseptica pagP* ($pagP_{BB}$) encodes a lipid A palmitoyl transferase that is responsible for the presence of palmitate in lipid A. The expression of $pagP_{BB}$ is regulated by the Bvg two-component system (13) that regulates the expression of many *Bordetella* genes that are involved in pathogenesis (14). $pagP_{BB}$ is maximally expressed in the Bvg-plus (Bvg^+) phase that is adopted when the system is active and includes the expression of many of the toxins and adhesins considered important for infection. When the Bvg system is inactive, the bacteria adopt the Bvg-minus (Bvg^-) phase, and the expression of these virulence genes is downregulated. Thus, the Bvg^+ and Bvg^- phases are regarded as the states that the bacteria adopt upon entering the host respiratory tract and the environment, respectively (14). We also showed that $pagP_{BB}$ is required for the persistence of *B. bronchiseptica* within the mouse respiratory tract through resistance to antibody-dependent complement-mediated killing (13, 15). This represented the first description of a

Received 20 August 2014 **Accepted** 14 November 2014

Accepted manuscript posted online 24 November 2014

Citation Hittle LE, Jones JW, Hajjar AM, Ernst RK, Preston A. 2015. *Bordetella parapertussis* PagP mediates the addition of two palmitates to the lipopolysaccharide lipid A. J Bacteriol 197:572–580. doi:10.1128/JB.02236-14.

Editor: V. J. DiRita

Address correspondence to R. K. Ernst, rkernst@umaryland.edu, or A. Preston, a.preston@bath.ac.uk.

Supplemental material for this article may be found at http://dx.doi.org/10.1128/JB.02236-14.

doi:10.1128/JB.02236-14

direct role for the *pagP* gene in virulence for *Bordetella*. *B. parapertussis* also contains a *pagP* gene, but *B. parapertussis* lipid A contains two secondary palmitates, compared to a single palmitate residue in *B. bronchiseptica* (16). Here we present characterization of *B. parapertussis pagP* ($pagP_{BPa}$), its role in lipid A biosynthesis, and the role of lipid A palmitoylation in *B. parapertussis* outer membrane function.

MATERIALS AND METHODS

Bacterial strains and plasmids. *Escherichia coli* XL1-Blue (Agilent Technologies, Wokingham, United Kingdom) or Top10 (Invitrogen Life Technologies, Paisley, United Kingdom) cells were used for cloning and maintenance of plasmids. *E. coli* SM10λ*pir* (17) or CC118λ*pir* was used as the donor strain in conjugations. The pCR2.1 Topo or pCR8 Gateway entry vector (Invitrogen Life Technologies) was used to clone PCR products. pEX100T (18) was used as a suicide vector for allelic-exchange mutagenesis in *B. parapertussis*. pBBR1kan is a derivative of pBBR1MCS in which the chloramphenicol resistance cassette has been replaced with a kanamycin resistance cassette. pBBR1MCS is a broad-host-range vector that is capable of replication in *Bordetella* (19). pBBR1kan was used to introduce a plasmid-borne *pagP* gene into the *B. parapertussis* wild type (WT) and the *pagP* mutant.

Bacterial growth media and conditions. *B. parapertussis* was grown on charcoal agar (BD, Oxford, United Kingdom) at 37°C. *E. coli* was grown on LB agar at 37°C. For liquid culture, *B. parapertussis* was grown in Stainer-Scholte broth (20) modified by the addition of Casamino Acids (50g liter^{-1}) at 37°C with shaking, and *E. coli* was grown in LB broth at 37°C with aeration. For growth of *B. parapertussis* in the Bvg$^-$ phase, $MgSO_4$ was added to growth medium to a concentration of 50 mM. Streptomycin (200 μg ml^{-1}), ampicillin (100 μg ml^{-1}), erythromycin (10 μg ml^{-1}), and kanamycin (50 μg ml^{-1}) were used where appropriate.

Chemicals and reagents. Chemicals and reagents were obtained from BD, Fisher Scientific (Loughborough, United Kingdom), or Sigma-Aldrich (Gillingham, United Kingdom).

DNA purification. Plasmid DNA was purified by using an Invitrogen plasmid DNA purification kit according to the manufacturer's instructions. Genomic DNA was purified by using the agarose plug method (21).

DNA manipulation. DNA manipulations were performed according to standard methods. DNA restriction and modifying enzymes were obtained from New England BioLabs (Hitchin, United Kingdom), Roche (Burgess Hill, United Kingdom), or Invitrogen Life Technologies.

PCR and primers. A genomic DNA template was made by resuspending plate-grown bacteria in 0.5 ml of water, boiling in a water bath for 5 min, spinning at top speed in a bench-top microcentrifuge for 2 min, and taking 0.2 ml of the supernatant. One microliter of supernatant was used per PCR. Each 50-μl PCR mixture was comprised of the genomic DNA template, buffer as directed by the manufacturer, deoxynucleoside triphosphates (dNTPs) (25 μM each), 20 ng of each primer, 5% (vol/vol) dimethyl sulfoxide (DMSO), 5 mM $MgCl_2$, and 2.5 units of *Taq* DNA polymerase (Promega, Southampton, United Kingdom). Primers used to amplify the *B. parapertussis pagP* locus were PagPF (5′-CTCCGCATTCC AGGTAGGCC-3′) and PagPR (5′-TTAGAACTCCCAGCGGCCAAAC-3′). PCR mixtures were incubated at 94°C for 5 min followed by 30 cycles of 94°C for 75 s, 60°C for 75 s, and 72°C for 90 s, followed by a final step at 72°C for 7 min.

Conjugations. Conjugations were performed as described previously (22).

Complementation of the *pagP* mutation. The region encompassing the putative *pagP* promoter and the *pagP* coding sequence was amplified from either *B. parapertussis* or *B. bronchiseptica* by PCR, and the PCR product was cloned into the pCR8/GW/Topo cloning vector. The insert was subcloned into pBBR1kan that had been modified to a Gateway destination vector by using the Invitrogen Gateway cloning system. This construct was introduced into *B. parapertussis* by conjugation.

SDS-PAGE/silver stain analysis of LPS. Whole-cell-lysate LPS samples were prepared and analyzed by sodium dodecyl sulfate (SDS)-PAGE/silver staining, as previously described (23).

Peptide killing assays. Bacteria were grown on agar plates for 3 days and then resuspended in phosphate-buffered saline (PBS). The suspensions were diluted to 10^4 bacteria/190 μl. Ten microliters of PBS containing C18G at a final concentration of 0, 1, 2.5, 5, or 10 μg ml^{-1} was added to each suspension, which was then incubated at 37°C for 30 min. Each peptide concentration was tested in triplicate. Suspensions were serially diluted in PBS, and 100 μl of dilutions was plated onto agar. Plates were incubated at 37°C for 3 days, and colonies were counted to enumerate the bacteria that had survived the assay. Differences in the numbers of surviving WT and mutant bacteria were compared by using a Student *t* test. The experiment was performed three times.

TLR4 stimulation assays. Reporter cell lines and stimulation assays were performed as described previously (20).

Lipid A structural analyses. (i) Matrix-assisted laser desorption ionization–time of flight/time of flight mass spectrometry. LPS was purified from 1 liter of cultures grown overnight, as described previously (24). Further treatment of LPS with RNase A, DNase I, and proteinase K ensured the removal of contaminating nucleic acids and proteins (25). Hydrolysis of LPS to isolate lipid A was accomplished with 1% SDS at pH 4.5, as described previously (26).

Lipid A was analyzed by matrix-assisted laser desorption ionization (MALDI) in the negative-ion mode on a 4700 proteomics analyzer (Applied Biosystems, Framingham, MA). Samples were dissolved in 10 μl of a mixture of 5-chloro-2-mercaptobenzothiazole (20 mg ml^{-1}) in chloroform-methanol-water (4:4:1, vol/vol/vol), and 0.5 μl of the sample was analyzed by MALDI-time of flight/time of flight mass spectrometry (TOF/TOF MS). Both MS and tandem MS (MS/MS) data were acquired in the reflectron mode with a neodymium-doped yttrium aluminum garnet (Nd:YAG) laser with a 200-Hz repetition rate, and up to 4,000 shots were accumulated for each spectrum. The precursor isolation window was set to ±5 Da. Tandem MS spectra were acquired with collision energies of 1 keV, and air was used as the collision gas. Instrument calibration and all other tuning parameters were optimized by using HP Calmix (Sigma-Aldrich, St. Louis, MO). Data were acquired and processed by using Data Explorer (Applied Biosystems, Framingham, MA).

(ii) Electrospray ionization linear ion trap Fourier transform ion cyclotron resonance mass spectrometry. Lipid A was analyzed by electrospray ionization (ESI) in the negative-ion mode on an linear trap quadrupole Fourier transform (LTQ-FT) mass spectrometer (Thermo Fisher, San Jose, CA). Samples were diluted to ~0.5 to 1.0 mg/ml in chloroform-methanol (1:1) and infused at a rate of 1.0 μl/min via a fused silica capillary (75-μm internal diameter [i.d.]; 360-μm outside diameter [o.d.]) with an ~30-μm spray tip (New Objective, Woburn, MA). Instrument calibration and tuning parameters were optimized by using a solution of Ultramark 1621 (Lancaster Pharmaceuticals, PA). For experiments acquired in the ion cyclotron resonance (ICR) cell, resolution was set to 100K, and ion populations were held constant by automatic gain control at 1.0×10^6 and 5.0×10^5 for MS and MS/MS, respectively. For tandem mass spectra, the precursor ion selection window was set to 5 Da, and the collision energy was set to 30% on the instrument scale. Data from the collision-induced dissociation (CID) MS^n analysis (where *n* represents the number of times an ion was subjected to MS) in the linear ion trap were acquired with an ion population of 1.0×10^4 and a maximum fill time of 200 ms. The subsequent MS^3 and MS^4 events had an isolation window of 4 Da with a collision energy of 25%. All spectra were acquired over a time period of 1 min and averaged. MS and MS^2 events were mass analyzed in the ICR cell, and MS^3 and MS^4 events were mass analyzed in the LTQ instrument. Data were acquired and processed by using Xcalibur, version 1.4 (Thermo Fisher), utilizing 7-point Gaussian smoothing.

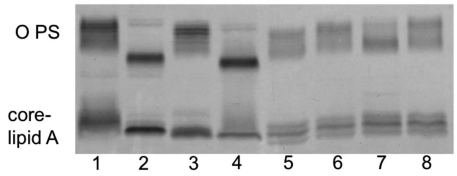

FIG 1 SDS-PAGE LPS profiles of the WT and a *B. parapertussis pagP* mutant grown in either the Bvg-plus or Bvg-minus phase and these strains carrying a plasmid-borne copy of either $pagP_{BPa}$ or $pagP_{BB}$ (Bvg-plus phase only). Lane 1, WT in the Bvg-plus phase; lane 2, WT in the Bvg-minus phase; lane 3, *B. parapertussis pagP* mutant in the Bvg-plus phase; lane 4, *B. parapertussis pagP* mutant in the Bvg-minus phase; lane 5, WT in the Bvg-plus phase with pBBR$pagP_{BPa}$; lane 6, *B. parapertussis pagP* mutant in the Bvg-plus phase with pBBR$pagP_{BPa}$; lane 7, WT in the Bvg-plus phase with pBBR$pagP_{BB}$; lane 8, *B. parapertussis pagP* mutant in the Bvg-plus phase with pBBR$pagP_{BB}$.

RESULTS

Identification of $pagP_{BPa}$. $pagP_{BPa}$ was identified by genome sequence analysis using the $PagP_{BB}$ sequence (Swiss-Prot database accession number Q7WFT9.1). The *B. parapertussis* and *B. pertussis* genes were found to be nearly identical at the DNA level in both the promoter and coding sequence. A single G:A base change in the middle position of the 24th codon was observed, which resulted in an aspartate in $PagP_{BPa}$, compared to a glycine in $PagP_{BB}$. To investigate the role of *pagP* in overall LPS biosynthesis in *B. parapertussis*, a *B. parapertussis pagP* mutant was constructed and analyzed by using SDS-PAGE to determine the LPS profile compared to that of the WT (Fig. 1).

In these analyses, two main LPS types are visible: lipid A-core LPS and lipid A-core that is further substituted with O polysaccharide (O PS). The WT LPS profile differed between the Bvg^+ and Bvg^- phases. In the plus phase, core-lipid A LPS migrated as a diffuse smear, indicative of a heterogeneous nature of LPS structures being present in this region. The O PS-containing LPS separated as a series of bands, demonstrating that LPS molecules that differ in the number of O PS repeats were well separated (Fig. 1, lane 1). In the Bvg^- phase, the O PS migrated as a compacted series of bands due to the action of the Bvg^--phase enzyme WbmE, which deaminates some of the O PS uronamide sugars (27). In addition, the core-lipid A LPS was present as a single intense band and just one or two other very faint bands, suggesting that a restricted number of core-lipid A structures were expressed in the minus phase compared to the plus phase (Fig. 1, lane 2).

The LPS profile of the $pagP_{BPa}$ mutant differed from that of the WT in the core-lipid A region. In the Bvg^+ phase, the mutant profile comprised a doublet with near-equal-intensity bands, whereas in the minus phase, a single band was observed (Fig. 1, lanes 3 and 4). This suggests that $PagP_{BPa}$ expression is required for some of the core-lipid A structures observed in the WT and that Bvg activity affects the expression of PagP-dependent LPS structures. Importantly, these analyses demonstrate that mutant structures are incorporated into mature LPS and are likely incorporated into the outer membrane. This is important for interpreting the phenotype of the $pagP_{BPa}$ mutant (see below).

To confirm the role of $pagP_{BPa}$ in LPS biosynthesis, the *pagP* mutation was complemented in *trans* by expressing *pagP* from a plasmid using the native *pagP* promoter. The LPS profile of the complemented mutant in the Bvg^+ phase comprised three well-resolved core-lipid A bands (Fig. 1, lane 6). This is different from the WT profile. We hypothesized that the multicopy nature of carrying the complementing gene on a plasmid was responsible for this difference. Thus, the complemented mutant profile was compared to that of the WT carrying the plasmid copy of *pagP* (Fig. 1, lane 5) and found to be the same. These data support the conclusion that the loss of core-lipid A bands from the profile of the $pagP_{BPa}$ mutant was due to a mutation of *pagP* (see also below).

Mass spectrometric analysis of lipid A isolated from WT *B. parapertussis* LPS. To define the specific structural differences between WT and mutant LPS structures, lipid A was purified from both strains and analyzed by mass spectrometry (MS). MALDI TOF/TOF and ESI LTQ-FT MS platforms were used to gain comprehensive structure determination. The negative-ion-mode MALDI-TOF mass spectrum of lipid A isolated from WT *B. parapertussis* LPS is shown in Fig. 2A. The most abundant ion, at *m/z* 1,332 (Fig. 2A), corresponded to a singly deprotonated lipid A structure that contained two phosphate groups and four acyl chains (i.e., diphosphoryl tetra-acylated lipid A). Two other prominent singly charged ions were recorded at *m/z* values of 1,570 (diphosphoryl penta-acylated lipid A) and 1,808 (diphosphoryl hexa-acylated lipid A). The ions at *m/z* 1,570 and 1,808 differed from the ion at *m/z* 1,332 by the addition of one and two secondary palmitate (C_{16}) acyl chains, respectively. The proposed lipid A structures for the ions at *m/z* 1,332, 1,570, and 1,808 are displayed in Fig. 2. Structure determination was based on the tandem mass spectrometry experiments discussed in detail below. In addition to the *m/z* values mentioned above, a number of other *m/z* values were observed, which demonstrated the extensive heterogeneity of lipid A structures present in lipid A isolated from WT *B. parapertussis* LPS (Fig. 2A). These *m/z* values corresponded to differing phosphorylation and acylation patterns (see Table S1 in the supplemental material for proposed structures of these additional ions).

Mass spectrometric analysis of lipid A isolated from *B. parapertussis pagP* mutant LPS. The negative-ion-mode MALDI-TOF mass spectrum of lipid A isolated from *B. parapertussis pagP* mutant LPS is shown in Fig. 2B. This lipid A also displayed the most abundant ion, at *m/z* 1,332 (Fig. 2B), which corresponded to a singly deprotonated diphosphoryl tetra-acylated lipid A structure. Of particular note, ions at *m/z* 1,570 and 1,808, corresponding to the addition of one and two secondary C_{16} acyl chains, respectively, were not present in mutant lipid A. All *m/z* values for mutant lipid A were also observed for lipid A from WT LPS and corresponded to identical structures (see Table S1 in the supplemental material).

Determination of acyl chain positioning in lipid A isolated from WT and *B. parapertussis pagP* mutant LPS using tandem mass spectrometry. In order to confidently assign structures to specific *m/z* values, a series of tandem MS experiments using a MALDI-TOF/TOF mass spectrometer were performed. In addition, multistage tandem MS (MS^n) experiments were performed on an ESI LTQ-FT MS platform to further validate structure assignment. The gas-phase dissociation of the precursor ion at *m/z* 1,332 determined via the MALDI-TOF/TOF platform revealed structure-specific, diagnostic product ions that allowed confident assignment of the four acyl chains along the lipid A glucosamine disaccharide (Fig. 3A). Gas-phase dissociation for structure determination of lipid A via tandem mass spectrometry, whereby structure-specific, diagnostic product ions are used for structure determination, was reported previously (12, 28). Of note, the collective

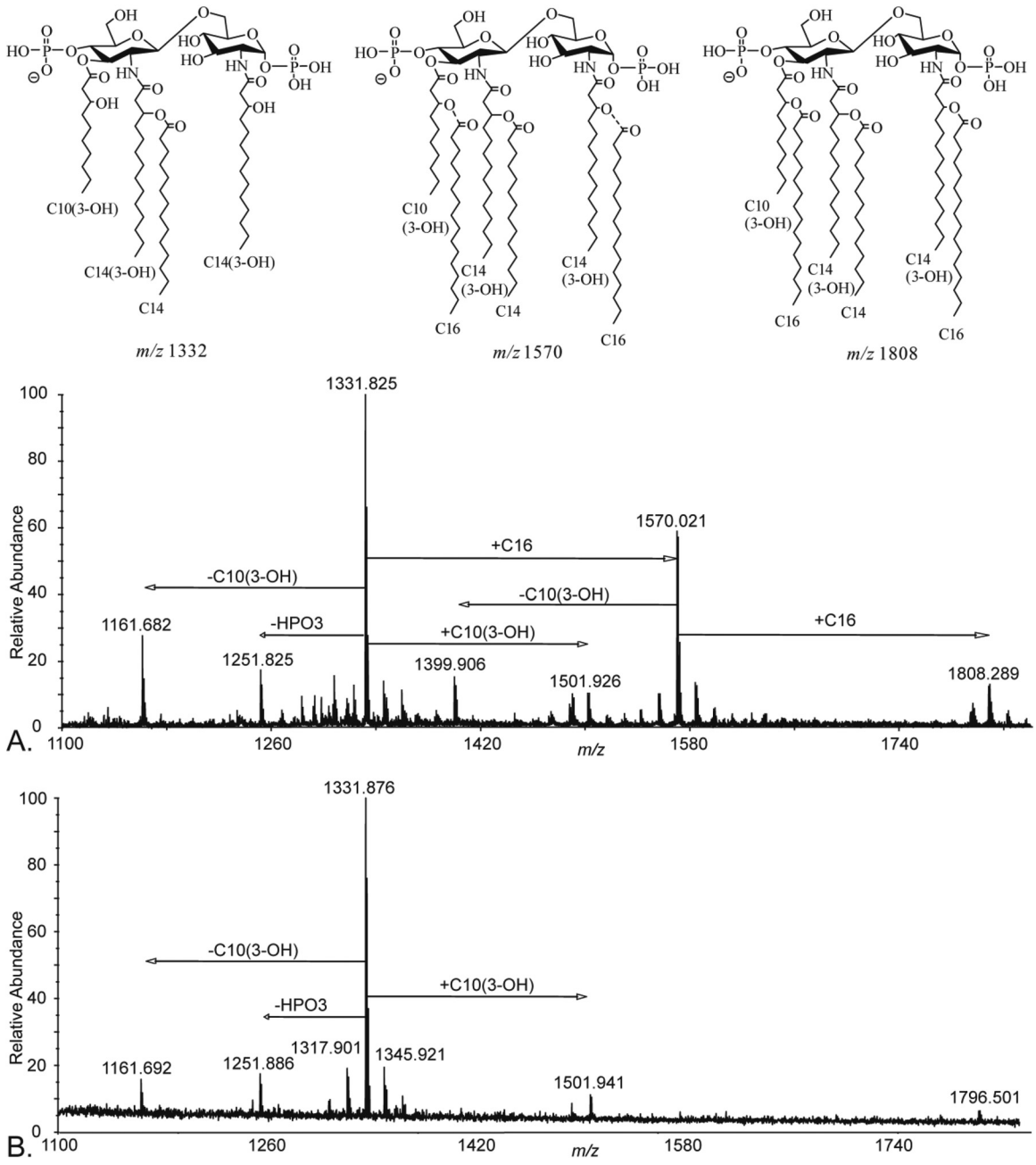

FIG 2 Negative-ion-mode MALDI-TOF mass spectra of lipid A isolated from LPS from the WT (A) and the *B. parapertussis pagP* mutant (B). Ions at *m/z* 1,570 and 1,808 represent the addition of one and two 2° C_{16} acyl chains to the ion at *m/z* 1,332, respectively. These ions are absent from the mutant lipid A spectrum. C_{16}, palmitic acid; C_{10}(3-OH), 3-hydroxy capric acid; HPO_3, phosphate group. Proposed lipid A structures at *m/z* values of 1,332, 1,570, and 1,808 are displayed. In the *m/z* 1,570 structure, the dashed lines indicate that the palmitate is present as a 2° acyl chain at either the C-2 or C-3′ position; i.e., the structure is penta-acylated.

analysis of several cross-ring, glycosidic, and competitive neutral losses of 1° acyl chains yielded a consistent pattern where the four acyl chains were confidently assigned to the following positions: amide-linked C_{14}(3-OH) at the C-2 and C-2′ positions, ester-linked C_{10}(3-OH) at the C-3′ position, and a secondary C_{14} ester linked via the 3-hydroxy position of the C-2 acyl chain (Fig. 2, structure at *m/z* 1,332). For example, the product ion at *m/z* 948.5 corresponded to a $^{0,2}A_2$ cross-ring fragment that localized the 1° C_{10}(3-OH) and C_{14}(3-OH) acyl chains and the 2° C_{14} acyl chain to the distal (nonreducing) end of the disaccharide. Cross-ring and glycosidic product ions were named according to the nomenclature outlined by Domon and Costello (29), with the slight modification of designating the loss of neutral acyl chains if applicable. Next, the cross-ring product ion at *m/z* 796.4 [$^{0,2}A_2$-C_{10}(3-OH)ket], presumably a consecutive dissociation from the ion at *m/z* 948.5, corresponded to the neutral loss of the 1° C_{10}(3-OH) as a ketene from the $^{0,2}A_2$ ion. These product ions determined that the C-3′ position is occupied by the 1° C_{10}(3-OH) acyl

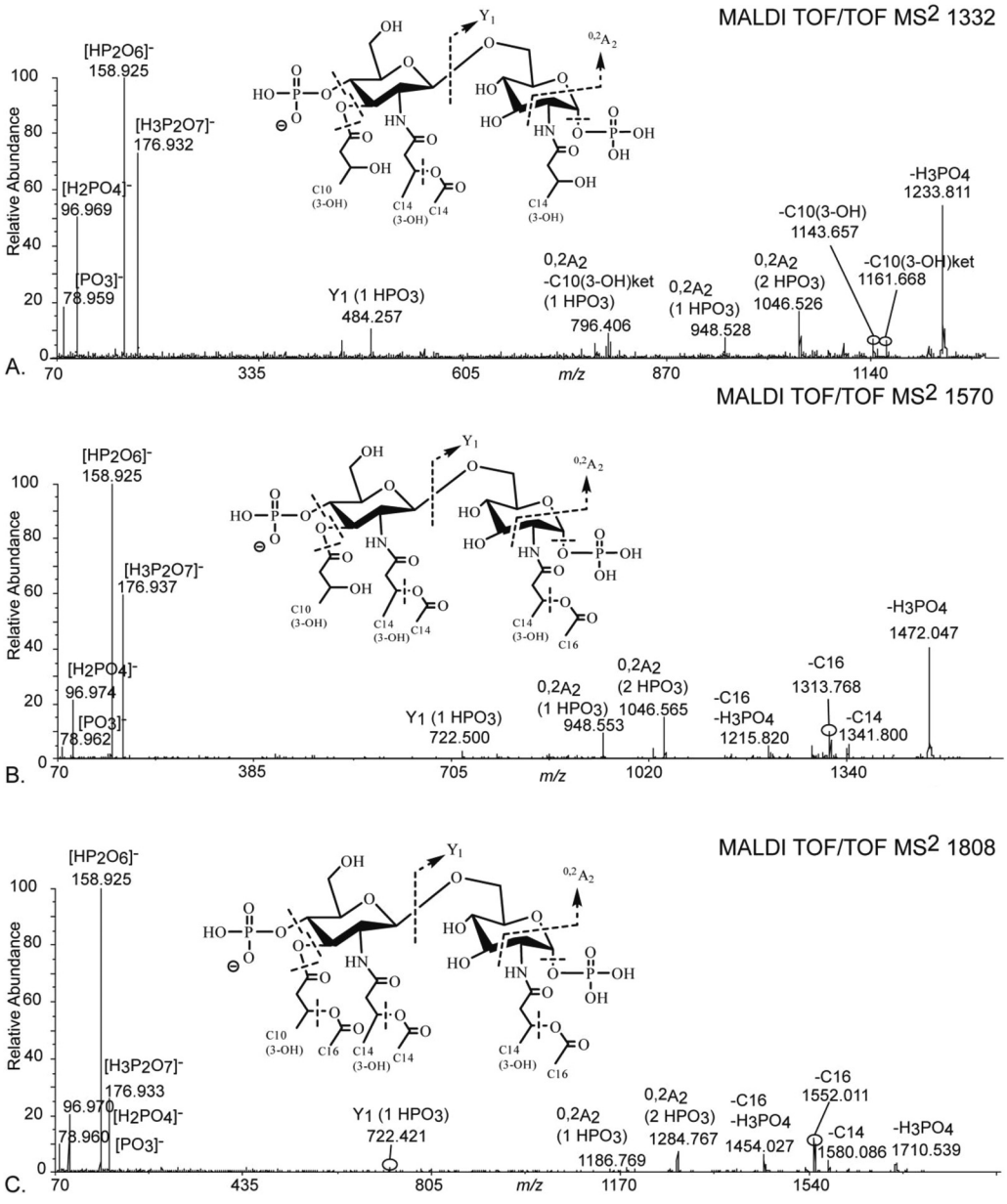

FIG 3 Negative-ion-mode MALDI-TOF/TOF mass spectra for precursor ions at *m/z* 1,332 (A), *m/z* 1,570 (B), and *m/z* 1,808 (C) isolated from WT *B. parapertussis* lipid A. Proposed lipid A structures for each precursor ion are shown in each spectrum, with dashed lines representing possible cleavage sites. Diagnostic cross-ring and glycosidic product ions provided unambiguous structure assignment and were named according to the nomenclature outlined by Domon and Costello (29), with the slight modification of designating the number of phosphate groups present and the loss of neutral acyl chains if applicable. All precursor ions were diphosphorylated with a heterogeneous mixture of bisphosphate and pyrophosphate. Only the bisphosphate configuration is displayed. C_{16}, palmitic acid; C_{10}(3-OH), 3-hydroxy capric acid; C_{10}(3-OH)ket, neutral loss as a ketene; HPO_3, phosphate; H_3PO_4, phosphoric acid; $[H_3P_2O_7]^-$ and $[HP_2O_6]^-$, pyrophosphate product ions; $[H_2PO_4]^-$ and $[PO_3]^-$, phosphate product ions.

chain and that the C-2′ position contained the 1° C_{14}(3-OH) and 2° C_{14} acyl chains. In addition, the glycosidic product ion at *m/z* 484.2 (Y_1) squarely indicated that the reducing end of the lipid A disaccharide contained a 1° C_{14}(3-OH) at the C-2 position. Further confirmation of the structure assignment for the ion at *m/z* 1,332 was demonstrated via the use of tandem mass spectrometry using an ESI LTQ-FT mass spectrometer, where MS^n experiments were performed (see Fig. S1 in the supplemental material). The precursor ions at *m/z* 1,332 from both the WT and the *pagP* mutant had identical structures.

Structure assignment for the precursor ion at *m/z* 1,570 corresponded to a diphosphoryl penta-acylated lipid A with acyl chain assignment as follows: amide-linked C_{14}(3-OH) at the C-2 and C-2′ positions, ester-linked C_{10}(3-OH) at the C-3′ position, secondary C_{14} ester linked via the 3-hydroxy position of the C-2 acyl chain, and one secondary C_{16} ester linked via the 3-hydroxy position of the C-2 or the C-3′ acyl chain (Fig. 2, structure at *m/z* 1,570). As described above for the precursor ion at *m/z* 1,332, diagnostic product ions which included cross-ring, glycosidic, and competitive neutral losses of acyl chains were identified and used to

confidently assign the structure of the ion at *m/z* 1,570 (see Fig. 3B for identities and *m/z* values of several diagnostic product ions). Of particular note, the 2° C_{16} acyl chain appeared to be localized to the reducing end (C-2 position), yet conclusive evidence for the exclusive positioning of the C_{16} acyl chain was not obtained via MALDI-TOF/TOF experiments. Further experiments using an ESI LTQ-FT mass spectrometer capable of higher-order MS^n revealed that the 2° C_{16} acyl chain was localized to either the C-2 or C-3′ position (see Fig. S2 in the supplemental material). Given the inherent difficulty of determining even relative amounts of isomeric structures during ESI mass spectrometry experiments, determination of the abundance of structures having a secondary C_{16} at either the C-2 position or the C-3′ position was not attempted.

Structure assignment for the precursor ion at *m/z* 1,808 corresponded to a diphosphoryl hexa-acylated lipid A with acyl chain assignment as follows: amide-linked C_{14}(3-OH) at the C-2 and C-2′ positions, ester-linked C_{10}(3-OH) at the C-3′ position, secondary C_{14} ester linked via the 3-hydroxy position of the C-2 acyl chain, and two secondary C_{16} acyl chains ester linked via the 3-hydroxy position of the C-2 and C-3′ acyl chains (Fig. 2, structure at *m/z* 1,808). Evidence and reasoning analogous to those for the precursor ions at *m/z* 1,332 and 1,570 were used to determine the structure of this ion (Fig. 3C; see also Fig. S3 in the supplemental material). In effect, diagnostic product ions were identified to confidently assign the positions of the two 2° C_{16} acyl chains.

These data demonstrate that *B. parapertussis* lipid A contains molecules with either one or two palmitates and that the presence of palmitate is dependent on $pagP_{BPa}$. In turn, this strongly suggests that *B. parapertussis* PagP transfers two palmitate moieties to lipid A. This is different from *B. bronchiseptica* PagP, which transfers only a single palmitate. It was possible that the two enzymes have different transferase abilities, presumably arising from the single-amino-acid difference between the two enzymes, or that the different lipid A substrates encountered by the enzymes in the two hosts direct different transferase activities. To investigate this, $PagP_{BB}$ was expressed in the *B. parapertussis pagP* mutant. The *B. bronchiseptica* gene was carried on a plasmid and expressed from its natural promoter (the promoter regions of *B. bronchiseptica* and *B. parapertussis* are identical). This construct was previously used to complement a *B. bronchiseptica pagP* mutation (13). Complementation of the *B. parapertussis pagP* mutation by $pagP_{BB}$ resulted in a lipid A-core profile identical to that produced by complementation with $pagP_{BPa}$ (Fig. 1, lanes 7 and 8), suggesting that both the *B. parapertussis* and *B. bronchiseptica* enzymes have the same activity in the *B. parapertussis* background. To confirm this, lipid A was purified from both complemented strains and analyzed by MS (Fig. 4). For both lipid A preparations, ions that corresponded to molecules containing either a single or two palmitate additions were detected, demonstrating that $PagP_{BB}$ can add two palmitates to *B. parapertussis* lipid A. Thus, both $PagP_{BB}$ and $PagP_{BPa}$ and have dual functionality, in that they can add palmitate to two different sites in lipid A. $PagP_{BB}$ does this in *B. parapertussis* but not in *B. bronchiseptica*, and thus, we propose that the dual functionality is directed by the *B. parapertussis* lipid A acceptor substrate.

***pagP*$_{BPa}$ is required for WT levels of resistance to C18G.** The acylation pattern of lipid A is an important determinant of the integrity of the outer membrane of Gram-negative bacteria. In turn, this is important for a range of functions, including resisting antimicrobial molecules produced by hosts during infection. We

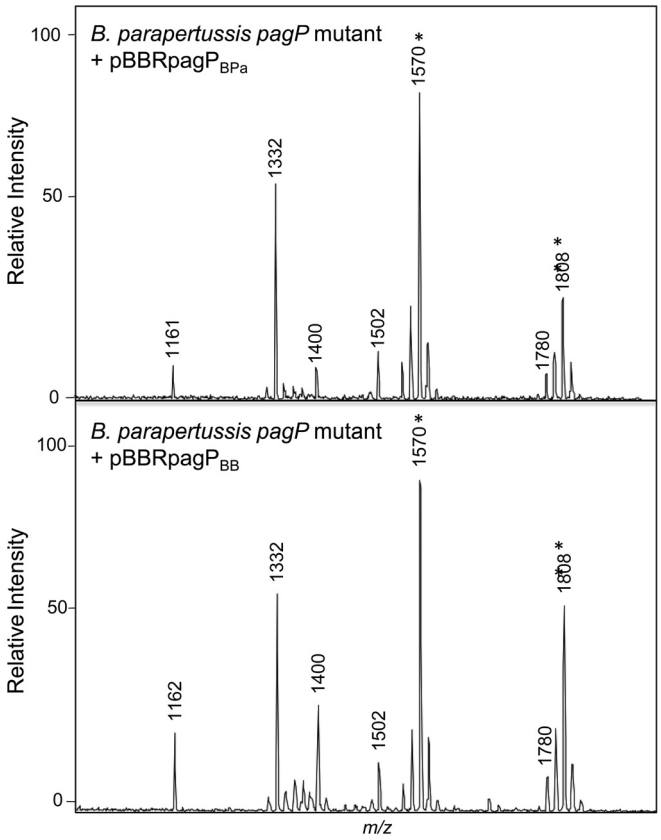

FIG 4 Mass spectra of the lipid A's of *B. parapertussis pagP* complemented with either $pagP_{BPa}$ (A) or $pagP_{BB}$ (B). Ions corresponding to lipid A with a single palmitate are indicated by * (*m/z* 1,570), and those with two palmitates are indicated by ** (*m/z* 1,808). Both strains produced identical lipid A's, demonstrating that both *B. parapertussis* PagP and *B. bronchiseptica* PagP have dual functionality.

hypothesized that $pagP_{BPa}$ contributes to the ability of the bacterium to resist host antimicrobial peptides, as observed for other bacterial species. To test this, we measured the level of killing of the WT and the *B. parapertussis pagP* mutant after exposure to C18G, a synthetic α-helical antimicrobial peptide (30). Approximately 1×10^4 CFU of the WT or mutant were incubated with the peptide (0 to 10 μg ml^{-1}) for 30 min at 37°C, and the number of surviving bacteria was enumerated. The results from a representative experiment are shown in Fig. 5. At each concentration of peptide, a significantly greater number of mutant bacteria than WT bacteria were killed. Overall, our data demonstrate that the WT level of resistance to C18G-mediated killing is dependent on $pagP_{BPa}$.

TLR4 stimulation assays. A key activity of lipid A during infection is stimulation of TLR4-mediated signaling. The acylation pattern of lipid A is a key determinant of this activity. The relative potencies for stimulation of TLR4-mediated signaling of lipid A isolated from the WT and *pagP* mutant strains were measured. A recombinant reporter system was used (20), expressing either human or murine TLR4 signaling complexes, as these two systems recognize and respond to different lipid A structures differently. Unstimulated cells acted as a negative control. Stimulation with a known agonist of NF-κB-mediated signaling, interleukin-1 (IL-1), resulted in relative light unit (RLU) values of 0.54 ± 0.03 and

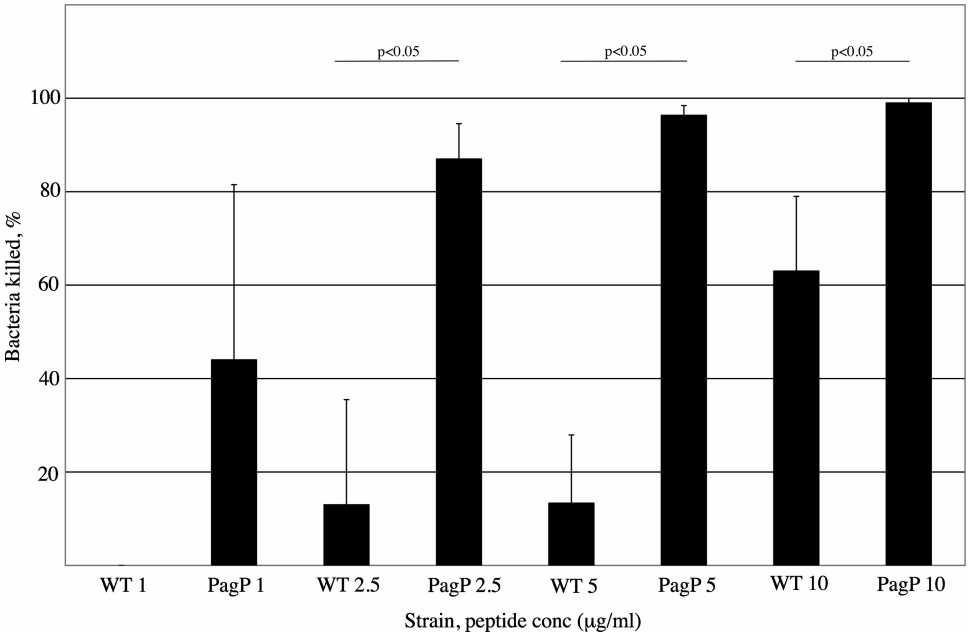

FIG 5 *B. parapertussis pagP* is more susceptible to killing by the synthetic antimicrobial peptide C18G than the WT. A significantly different level of killing of the WT compared to the *pagP* mutant was observed. This was observed in three independent experiments; data from a representative experiment are shown here.

0.59 ± 0.05 for murine and human TLR4-mediated signaling, respectively, demonstrating the responsiveness of the system. Stimulation with an *E. coli* lipid A (1,000 ng/ml) biosynthetic intermediate, lipid IV_A, which is a strong agonist of murine but not of human TLR4 signaling, resulted in RLU values of 0.36 ± 0.03 and 0.05 ± 0.00 for murine and human TLR4-mediated signaling, respectively, and demonstrated that the experimental system could detect species-specific stimulation.

B. parapertussis WT lipid A was a more potent stimulant of murine than of human TLR4-mediated signaling (Fig. 6). *pagP* mutant lipid A was significantly less potent than the WT for stimulation of both murine (Fig. 6A) and human (Fig. 6B) TLR4-mediated signaling but was particularly attenuated for the human-derived system. These data demonstrate that $PagP_{BPa}$-mediated modification of *B. parapertussis* lipid A significantly alters the endotoxin activity of lipid A toward the human TLR4 signaling complex.

DISCUSSION

Previously, we characterized *B. bronchiseptica* PagP as a Bvg-regulated lipid A palmitoyl transferase and determined that PagP-mediated palmitoylation was required for resistance to antibody-dependent complement-mediated killing (13, 15). Here we show that *B. parapertussis* PagP is also a Bvg-regulated lipid A palmitoyl transferase but one that is able to transfer two palmitates to lipid A, a novel finding. When expressed in *B. parapertussis*, $PagP_{BB}$ also mediates the addition of two palmitates to lipid A. We propose that the lipid A acceptor substrate of *B. parapertussis* directs this dual functionality.

Interestingly, the MS analyses presented here demonstrated

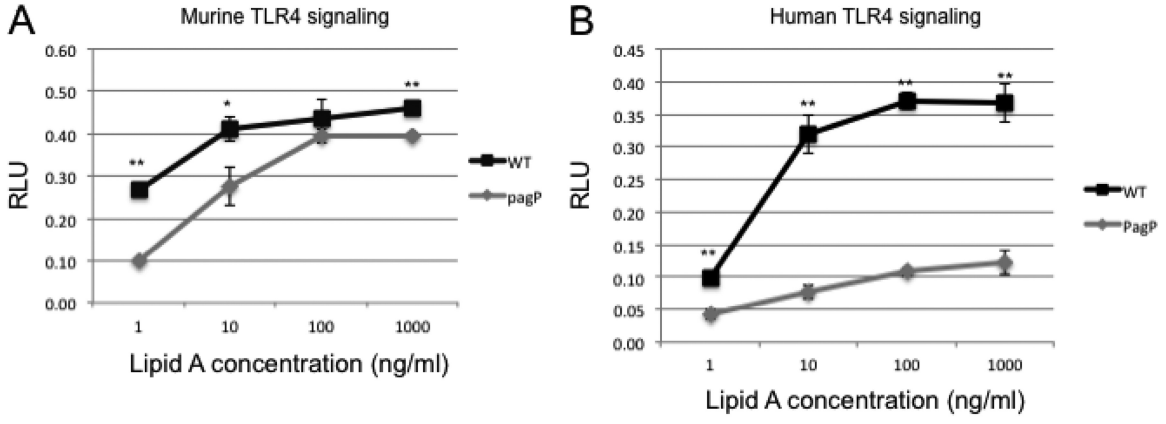

FIG 6 Stimulation of murine or human TLR4-mediated signaling by WT and *B. parapertussis* lipid A. Both lipid A's were more potent stimulators of murine than of human TLR4-mediated signaling; however, *B. parapertussis pagP* lipid A was significantly less potent than that of the WT, particularly for the activation of human TLR4. *, $P < 0.05$; **, $P < 0.001$.

considerable lipid A heterogeneity in addition to palmitoylation. Variability in the presence of C_{10}(3-OH) was observed (Fig. 2). Ions at *m/z* 1,162 and 1,400 corresponded to derivatives of the major tetra- and penta-acylated molecules lacking C_{10}(3-OH), whereas the ion at *m/z* 1,502 corresponded to a derivative of the tetra-acylated molecule that contained an additional C_{10}(3-OH), presumably at the C-3 position as a result of incomplete deacylation by PagL (12). Furthermore, each of the peaks corresponding to the tetra-, penta-, and hexa-acylated species was surrounded by a series of peaks, each differing from the next by 14 mass units (Fig. 2), corresponding to a series of structures, each differing by one methylene (CH_2) unit. This suggests that *B. parapertussis* incorporates a range of different acyl chains into its lipid A, including those containing an odd number of carbon atoms. *Bordetella* LpxA has relaxed acyl chain specificity that may contribute to this heterogeneity (31). In turn, this suggests that *B. parapertussis* lipid A contains not only three major molecular species but also numerous acylation variants of these major species. A full structural characterization of this heterogeneity is under way.

$PagP_{BPa}$ mediates the conversion of tetra-acylated to penta- and hexa-acylated lipid A and thus alters the properties of the outer membrane. A *pagP* mutant was more susceptible to direct killing by an α-helical antimicrobial peptide (C18G), suggesting that a loss of palmitoylation affects the integrity or fluidity of the outer membrane. This has also been observed for *Salmonella enterica* serovar Typhimurium, where a *pagP* mutant displayed increased outer membrane permeability in response to C18G (32).

PagP-mediated palmitoylation results in an altered potency of *B. parapertussis* lipid A for stimulating signaling via TLR4. WT lipid A was more proinflammatory than *pagP* mutant lipid A, particularly via the human-derived signaling complex. When considering the basis for the effect of palmitoylation on lipid A potency, it is important to consider that the individual lipid A preparations are comprised of a mixture of lipid A molecules and that the overall potency is the sum of their individual potencies, which may include some antagonistic activities. Either way, the Bvg-regulated expression of $pagP_{BPa}$ appears to confer on *B. parapertussis* a mechanism by which to regulate the potency of its lipid A for TLR4 stimulation. The Bvg^+ phase, in which $PagP_{BPa}$ appears to be maximally expressed, is thought to be that adopted by the bacteria during infection. In this case, our data suggest that both singly and doubly palmitoylated lipid A will be synthesized and that lipid A is at its most potent, compared to the Bvg-minus phase. However, *B. parapertussis* has low-potency lipid A compared to that of *B. bronchiseptica*, and it has been demonstrated in mice that *B. parapertussis* avoids invoking host immune responses through the lack of stimulation of TLR4-mediated signaling (33). This suggests that Bvg-mediated regulation of lipid A potency does not play a role during infection.

Clearly, the *in vitro* system used here does not reveal the precise immune response stimulated by either palmitoylated or nonpalmitoylated lipid A during infection, and thus, the consequences of regulating the level of lipid A palmitoylation are not clear. In addition, our data demonstrate that PagP activity regulates outer membrane function in other ways, such as resistance to host antimicrobial peptides, and that the bacterium may have to balance increased lipid A potency for TLR4 stimulation versus inherent resistance to immune effector molecules. In support of this, *B. bronchiseptica pagP* is required for persistent colonization of the mouse respiratory tract (13). However, a $pagP_{BB}$ mutant appears to colonize similarly to the WT during the early course of infection, with attenuation manifesting only between days 3 and 7 postinoculation, perhaps suggesting that there is little difference in early events when innate immunity resulting from TLR4 stimulation is operational. Furthermore, we demonstrated that $pagP_{BB}$ is required for resistance to antibody-dependent complement-mediated lysis (15), suggesting that the major role of *pagP* in *B. bronchiseptica* is to contribute to the integrity of the outer membrane.

It is also of interest to consider the difference in lipid A biosynthetic enzymes between *Bordetella* subspecies. *B. pertussis*, *B. bronchiseptica*, and *B. parapertussis* share a very similar set of lipid A biosynthesis and modification genes, but they each synthesize species-specific lipid A's (34). Some genes are mutated in one species (e.g., *pagP* in *B. pertussis* [13]), while subtle allelic differences result in differences in activity among species, e.g., *lpxA* (31). Here our data suggest that slight alterations in the lipid A structure can direct different activities of enzymes common to more than one species. Presumably, the evolution of these three species in their different niches and different infection biologies has selected for these subtly different combinations of lipid A biosynthesis activities. Thus, while the regulated expression of *Bordetella pagP* suggests that *B. parapertussis* may modulate its lipid A structure during infection, the extent to which this happens and the consequences of it require analyses *in vivo*, with consideration of the different potencies of stimulation of *B. parapertussis* lipid A toward TLR4 from different hosts.

ACKNOWLEDGMENT

This work was supported in part by a National Institutes of Health grant (1U54 AI57141) (R.K.E.).

REFERENCES

1. **Cherry JD.** 1992. Pertussis—the trials and tribulations of old and new pertussis vaccines. Vaccine **10:**1033–1038. http://dx.doi.org/10.1016/0264-410X(92)90113-X.
2. **Cherry JD.** 1996. Historical review of pertussis and the classical vaccine. J Infect Dis **174**(Suppl 3)**:**S259–S263.
3. **Heininger U, Stehr K, Schmittgrohe S, Lorenz C, Rost R, Christenson PD, Uberall M, Cherry JD.** 1994. Clinical characteristics of illness caused by *Bordetella parapertussis* compared with illness caused by *Bordetella pertussis*. Pediatr Infect Dis J **13:**306–309. http://dx.doi.org/10.1097/00006454-199404000-00011.
4. **Nennig ME, Shinefield HR, Edwards KM, Black SB, Fireman BH.** 1996. Prevalence and incidence of adult pertussis in an urban population. JAMA **275:**1672–1674. http://dx.doi.org/10.1001/jama.1996.03530450062034.
5. **Pichichero ME, Treanor J.** 1997. Economic impact of pertussis. Arch Pediatr Adolesc Med **151:**35–40. http://dx.doi.org/10.1001/archpedi.1997.02170380039006.
6. **Watanabe M, Nagai M.** 2004. Whooping cough due to *Bordetella parapertussis*: an unresolved problem. Expert Rev Anti Infect Ther **2:**447–454. http://dx.doi.org/10.1586/14787210.2.3.447.
7. **Mattoo S, Cherry JD.** 2005. Molecular pathogenesis, epidemiology, and clinical manifestations of respiratory infections due to *Bordetella pertussis* and other *Bordetella* subspecies. Clin Microbiol Rev **18:**326–382. http://dx.doi.org/10.1128/CMR.18.2.326-382.2005.
8. **Zhang X, Rodriguez ME, Harvill ET.** 2009. O antigen allows *B. parapertussis* to evade *B. pertussis* vaccine-induced immunity by blocking binding and functions of cross-reactive antibodies. PLoS One **4:**e6989. http://dx.doi.org/10.1371/journal.pone.0006989.
9. **Luderitz O, Galanos C, Lehmann V, Nurminen J, Rietschel ET, Rosenfelder G, Simon M, Westphal O.** 1973. Lipid A: chemical structure and biological activity. J Infect Dis **128:**S17–S29. http://dx.doi.org/10.1093/infdis/128.Supplement_1.S17.
10. **Akira S, Takeda K.** 2004. Toll-like receptor signalling. Nat Rev Immunol **4:**499–511. http://dx.doi.org/10.1038/nri1391.

11. **Caroff M, Aussel L, Zarrouk H, Martin A, Richards JC, Therisod H, Perry MB, Karibian D.** 2001. Structural variability and originality of the *Bordetella* endotoxins. Innate Immun **7:**63–68. http://dx.doi.org/10.1177/096805190100700111101.
12. **MacArthur I, Jones JW, Goodlett DR, Ernst RK, Preston A.** 2011. Role of *pagL* and *lpxO* in *Bordetella bronchiseptica* lipid A biosynthesis. J Bacteriol **193:**4726–4735. http://dx.doi.org/10.1128/JB.01502-10.
13. **Preston A, Maxim E, Toland E, Pishko EJ, Harvill ET, Caroff M, Maskell DJ.** 2003. *Bordetella bronchiseptica* PagP is a Bvg-regulated lipid A palmitoyl transferase that is required for persistent colonization of the mouse respiratory tract. Mol Microbiol **48:**725–736. http://dx.doi.org/10.1046/j.1365-2958.2003.03484.x.
14. **Cotter PA, Miller JF.** 2001. *Bordetella*, p 619–674. *In* Groisman E (ed), Principles of bacterial pathogenesis. Academic Press, San Diego, CA.
15. **Pilione MR, Pishko EJ, Preston A, Maskell DJ, Harvill ET.** 2004. *pagP* is required for resistance to antibody-mediated complement lysis during *Bordetella bronchiseptica* respiratory infection. Infect Immun **72:**2837–2842. http://dx.doi.org/10.1128/IAI.72.5.2837-2842.2004.
16. **El Hamidi A, Novikov A, Karibian D, Perry MB, Caroff M.** 2009. Structural characterization of *Bordetella parapertussis* lipid A. J Lipid Res **50:**854–859. http://dx.doi.org/10.1194/jlr.M800454-JLR200.
17. **Simon R, Priefer U, Pühler A.** 1982. A broad hostrange mobilisation system for in vivo genetic engineering: transposon mutagenesis in Gram negative bacteria. Biotechnology **1:**784–791.
18. **Schweizer HP, Hoang TT.** 1995. An improved system for gene replacement and XylE fusion analysis in *Pseudomonas aeruginosa*. Gene **158:**15–22. http://dx.doi.org/10.1016/0378-1119(95)00055-B.
19. **Kovach ME, Phillips RW, Elzer PH, Roop RM, II, Peterson KM.** 1994. pBBR1MCS: a broad-host-range cloning vector. Biotechniques **16:**800–801.
20. **Darveau RP, Pham TT, Lemley K, Reife RA, Bainbridge BW, Coats SR, Howald WN, Way SS, Hajjar AM.** 2004. *Porphyromonas gingivalis* lipopolysaccharide contains multiple lipid A species that functionally interact with both Toll-like receptors 2 and 4. Infect Immun **72:**5041–5051. http://dx.doi.org/10.1128/IAI.72.9.5041-5051.2004.
21. **Sambrook J, Fritsch EF, Maniatis T.** 1989. Molecular cloning: a laboratory manual, 2nd ed. Cold Spring Harbor Laboratory Press, Cold Spring Harbor, NY.
22. **Preston A, Allen AG, Cadisch J, Thomas R, Stevens K, Churcher CM, Badcock KL, Parkhill J, Barrell B, Maskell DJ.** 1999. Genetic basis for lipopolysaccharide O-antigen biosynthesis in bordetellae. Infect Immun **67:**3763–3767.
23. **Preston A, Mandrell RE, Gibson BW, Apicella MA.** 1996. The lipooligosaccharides of pathogenic Gram-negative bacteria. Crit Rev Microbiol **22:**139–180. http://dx.doi.org/10.3109/10408419609106458.
24. **Westphal O, Jann K.** 1965. Bacterial lipopolysaccharides: extraction with phenol-water and further applications of the procedure. Methods Carbohydr Chem **5:**83–91.
25. **Fischer W, Koch HU, Haas R.** 1983. Improved preparation of lipoteichoic acids. Eur J Biochem **133:**523–530. http://dx.doi.org/10.1111/j.1432-1033.1983.tb07495.x.
26. **Caroff M, Tacken A, Szabo L.** 1988. Detergent-accelerated hydrolysis of bacterial endotoxins and determination of the anomeric configuration of the glycosyl phosphate present in the "isolated lipid A" fragment of the *Bordetella pertussis* endotoxin. Carbohydr Res **175:**273–282. http://dx.doi.org/10.1016/0008-6215(88)84149-1.
27. **King JD, Vinogradov E, Preston A, Li J, Maskell DJ.** 2009. Post-assembly modification of *Bordetella bronchiseptica* O polysaccharide by a novel periplasmic enzyme encoded by *wbmE*. J Biol Chem **284:**1474–1483. http://dx.doi.org/10.1074/jbc.M807729200.
28. **Jones JW, Shaffer SA, Ernst RK, Goodlett DR, Turecek F.** 2008. Determination of pyrophosphorylated forms of lipid A in Gram-negative bacteria using a multivaried mass spectrometric approach. Proc Natl Acad Sci U S A **105:**12742–12747. http://dx.doi.org/10.1073/pnas.0800445105.
29. **Domon B, Costello CE.** 1988. A systematic nomenclature for carbohydrate fragmentations in FAB-MS/MS spectra of glycoconjugates. Glycoconj J **5:**397–409. http://dx.doi.org/10.1007/BF01049915.
30. **Darveau RP, Blake J, Seachord CL, Cosand WL, Cunningham MD, Cassiano-Clough L, Maloney G.** 1992. Peptides related to the carboxyl terminus of human platelet factor IV with antibacterial activity. J Clin Invest **90:**447–455. http://dx.doi.org/10.1172/JCI115880.
31. **Sweet CR, Preston A, Toland E, Ramirez SM, Cotter RJ, Maskell DJ, Raetz CR.** 2002. Relaxed acyl chain specificity of *Bordetella* UDP-N-acetylglucosamine acyltransferases. J Biol Chem **277:**18281–18290. http://dx.doi.org/10.1074/jbc.M201057200.
32. **Guo L, Lim KB, Poduje CM, Daniel M, Gunn JS, Hackett M, Miller SI.** 1998. Lipid A acylation and bacterial resistance against vertebrate antimicrobial peptides. Cell **95:**189–198. http://dx.doi.org/10.1016/S0092-8674(00)81750-X.
33. **Wolfe DN, Buboltz AM, Harvill ET.** 2009. Inefficient Toll-like receptor-4 stimulation enables *Bordetella parapertussis* to avoid host immunity. PLoS One **4:**e4280. http://dx.doi.org/10.1371/journal.pone.0004280.
34. **MacArthur I, Mann PB, Harvill ET, Preston A.** 2007. IEIIS Meeting minireview. *Bordetella* evolution: lipid A and Toll-like receptor 4. J Endotoxin Res **13:**243–247. http://dx.doi.org/10.1177/0968051907082609.